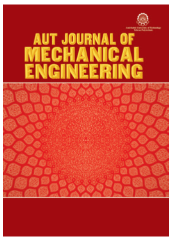

AUT Journal of Mechanical Engineering

AUT J. Mech. Eng., 3(1) (2019) 3-14
DOI: 10.22060/ajme.2018.14196.5712

Chebyshev Spectral Collocation Method for Flow and Heat Transfer in Magnetohydrodynamic Dissipative Carreau Nanofluid over a Stretching Sheet with Internal Heat Generation

M. G. Sobamowo[1*], L. O. Jayesimi[2], M. A. Waheed[3]

[1] Mechanical Engineering Department, University of Lagos, Lagos, Nigeria
[2] Works and Physical Planning Department, University of Lagos, Lagos, Nigeria
[3] Mechanical Engineering Department, Federal University of Agriculture, Abeokuta, Nigeria

ABSTRACT: In this paper, Chebyshev spectral collocation method is used to solve the unsteady two-dimensional flow and heat transfer of Carreau nanofluid over a stretching sheet subjected to magnetic field, temperature dependent heat source/sink and viscous dissipation. Similarity transformations are used to reduce the systems of the developed governing partial differential equations to nonlinear third and second orders ordinary differential equations which are solved by the numerical method. Good agreements are established between the results of the present numerical solution and the results of Runge-Kutta coupled with shooting method. Using kerosene as the base fluid embedded with the silver (Ag) and copper (Cu) nanoparticles, the effects of pertinent parameters on reduced Nusselt number, flow and heat transfer characteristics of the nanofluid are investigated and discussed. From the results, it is established temperature field and the thermal boundary layers of Ag-Kerosene nanofluid are highly effective when compared with the Cu-Kerosene nanofluid. Heat transfer rate is enhanced by increasing in power-law index and unsteadiness parameter. Skin friction coefficient and local Nusselt number can be reduced by magnetic field parameter and they can be enhanced by increasing the aligned angle. Friction factor is depreciated and the rate of heat transfer increases by increasing the Weissenberg number. It is hope that the present work will enhance the study of the flow and heat transfer processes.

Review History:

Received: 11 March 2018
Revised: 12 September 2018
Accepted: 12 September 2018
Available Online: 5 October 2018

Keywords:

MHD
Nanofluid
non-uniform heat source/sink
Carreau fluid and free convection

1- Introduction

The analysis of fluid flow and heat transfer over a stretching surface is very significant in controlling the quality of the end-product in various industrial applications such as wire and fiber coating, heat exchangers, extrusion process, polymer processing and chemical processing equipment, etc. Such processes have great dependence on the stretching and cooling rates [1]. Consequently, in the past few years, research efforts have been directed towards the analysis of this very important phenomenon of wide areas of applications. In an early study of MagnetoHydroDynamic (MHD) fluid flow over a stretching carried out by Anderson et al. [2, 3] effects of a power-law fluid caused by thin liquid film and magnetohydrodynamic on an unsteady stretching surface were investigated. Few years later, Chen [4] investigated the power-law fluid film flow of unsteady heat transfer stretching sheet while Dandapat et al. [5, 6] analyzed the effect of variable viscosity and thermo- capillarity on the heat transfer of liquid film flow over a stretching sheet. Meanwhile, Wang [7] developed an analytical solution for the momentum and heat transfer of liquid film flow over a stretching surface. Also, Chen [8] and Sajid et al. [9] investigated the flow characteristics of a non-Newtonian thin film over an unsteady stretching surface considering viscous dissipation using homotopy analysis and homotopy perturbation methods. After a year, Dandapat et al. [10] presented the analysis of two-dimensional liquid film flow over an unsteady stretching sheet while in the same year, effect of power-law index on unsteady stretching sheet was studied by Abbasbandy [11] while Santra and Dandapat [12] numerically studied the flow of the liquid film over an unsteady horizontal stretching sheet. A numerical approach was also used by Sajid et al. [13] to analyze the micropolar film flow over an inclined plate, moving belt and vertical cylinder. A year later, Noor and Hashim [14] investigated the effect of magnetic field and thermocapillarity on an unsteady flow of a liquid film over a stretching sheet while Dandapat and Chakraborty [15], and Dandapat and Singh [16] presented the thin film flow analysis over a non-linear stretching surface with the effect of transverse magnetic field. Heat transfer characteristics of the thin film flows considering the different channels have also been analyzed by Abdel-Rahman [17], Khan et al. [18], Liu et al. [19] and Vajaravelu et al. [20] Meanwhile, Liu and Megahad [21] used homotopy perturbation method to analyze thin film flow and heat transfer over an unsteady stretching sheet with internal heating and variable heat flux. Effect of thermal radiation and thermocapillarity on the heat transfer thin film flow over a stretching surface was examined by Aziz et al. [22]. In their study on the numerical simulation of Eyring Powell flow and unsteady heat transfer of a laminar liquid film over a stretching sheet using finite difference method, Khader and Megahed [23] established that increasing the Prandtl number reduces the temperature field across the thin film.

The promising significance of the MHD fluid behavior

Corresponding author, E-mail: mikegbeminiyi@gmail.com

in various engineering and industrial applications (such as in the design of cooling system with liquid metals, accelerators, MHD generators, nuclear reactor, pumps and flow meters and blood flow) still provokes the continuous studies and interests of researchers. Indisputably, numerous studies have been presented in literature on the behavior of magnetohydrodynamic flow in different flow configurations. Also, the effects of MHD on the non-Newtonian nanofluid have been of research interests in recent times. In a recent study, Lin et al. [24] examined the effect of MHD pseudo-plastic nanofluid flow and heat transfer film flow over a stretching sheet with internal heat generation. Numerically, Raju and Sandeep [25] studied heat and mass transfer in MHD non-Newtonian flow while Tawade et al. [26] presented the unsteady flow and heat transfer of thin film over a stretching surface in the presence of thermal radiation, internal heating in the presence of magnetic field. Heat and mass transfer of MHD flows through different channels have been analyzed [27-32]. Makinde and Animasaun [33] investigated the effect of cross diffusion on MHD bioconvection flow over a horizontal surface. In another study, Makinde and Animasaun [34] presented the MHD nanofluid on bioconvection flow of a paraboloid revolution with nonlinear thermal radiation and chemical reaction while Sandeep [35], Ramana Reddy et al. [36] and Ali et al. [37] studied the heat transfer behaviour of MHD flows.

The above studies have been the consequent of the various industrial and engineering applications of non-Newtonian fluids. Among the classes of non-Newtonian fluids, Carreau fluid which its rheological expressions was first introduced by Carreau [38], is one of the non-Newtonian fluids that its model is substantial for gooey, high and low shear rates [39]. On account of this headway, it has profited in numerous innovative and assembling streams [39]. Owing to these applications, different studies have been carried out to explore the characteristics of Carreau liquid in flow under different conditions. Hayat et al. [40] studied the influence of induced magnetic field and heat transfer on peristaltic transport of a Carreau fluid. Olajuwon [41] presented a study on MHD flow of Carreau liquid over vertical porous plate with thermal radiation. Hayat et al. [42] investigated the convectively heated flow of Carreau fluid while in the same year, Akbar et al. [43] analyzed the stagnation point flow of Carreau fluid. Also, Akbar [44] presented blood flow of Carreau fluid in a tapered artery with mixed convection. A year later, Mekheimer [45] investigated the unsteady flow of a carreau fluid through inclined catheterized arteries having a balloon with time-variant overlapping stenosis. Elmaboud et al. [46] developed series solution of a natural convection flow for a Carreau fluid in a vertical channel with peristalsis. Using a revised model, flow of Carreau nanoliquid in the presence of zero mass flux condition at the stretching sheet has been examined by Hashim and Khan [47]. Raju and Sandeep [29] explored heat and mass transfer in Falkner-Skan flow of Carreau liquid past a wedge. The MHD flow of Carreau fluid with thermal radiation and cross diffusion effects was investigated by Machireddy and Naramgari [48]. Sulochana et al. [49] provided an analysis of magnetohydrodynamic stagnation-point flow of a Carreau nanofluid. In recent time, Raju and Sandeep [27] put forward the problem of homogeneous-heterogeneous reactions in non-linear stretched flow of Casson-Carreau fluid. Hayat et al. [1] presented radiative flow of Carreau liquid in presence of Newtonian heating and chemical reaction. Kumar and Kumar [39] applied Runge-Kutta and Newton's method to analyze the flow and heat transfer of electrically conducting liquid film flow of Carreau nanofluid over a stretching sheet by considering the aligned magnetic field in the presence of space and temperature dependent heat source/sink, viscous dissipation and thermal radiation.

The fast rate of convergence and a very large converging speed of spectral methods over most of the commonly used numerical methods have been established in the field of numerical simulations. The converging speed of the approximated numerical solution to the primitive problem is faster than any one expressed by any power-index of $N-1$. Numerical methods such as Finite Element Method (FEM) and the Finite Volume Method (FVM) provide linear convergence, while, the spectral methods provide exponential convergence [50]. Spectral methods have been widely applied in computational fluid dynamics [51, 52], electrodynamics [53] and magnetohydrodynamics [54, 55]. Recent numerical work concerned with the solution of non-linear differential equations has also provided more and more evidence of the applicability and accuracy of the Chebyshev collocation method [56-61]. The main advantage of spectral methods lies in their accuracy for a given number of unknowns. For smooth problems in simple geometries, they offer exponential rates of convergence/spectral accuracy [62-65]. Despite the high accuracy and efficiency of the method, it has not been significantly applied to nonlinear heat transfer problems. In fact, to the best of the authors' knowledge, this method has not been applied to the analysis of flow and heat transfer of Carreau fluid. Therefore, in this study, Chebychev spectral collocation method is applied to analyze the flow and heat transfer of an electrically conducting liquid film flow of Carreau nanofluid over a stretching sheet subjected to magnetic field, temperature dependent heat source/sink and viscous dissipation. Using kerosene as the base fluid embedded with the silver (Ag) and copper (Cu) nanoparticles, the effects of pertinent parameters on reduced Nusselt number, flow and heat transfer characteristics of the nanofluids are investigated and discussed.

2- Problem Formulation

Consider an unsteady, two-dimensional boundary layer flow of an electrically conducting and heat generating Carreau nanofluid over a stretching sheet bounded by a thin liquid film of uniform thickness $h(t)$ over a horizontal elastic sheet which emerges from a narrow slit at the origin of the Cartesian coordinate system which is schematically represented in Fig. 1. The sheet is stretched along the x-axis with stretching velocity $U(x,t)$ and y–axis is normal to it. An inclined magnetic field. The effects of non-uniform heat source/sink, thermal radiation, viscous is applied to the stretching sheet at angle dissipation and volume fraction are taken into consideration. Following the assumptions, the equations for continuity and motion are [39]

$$\frac{\partial u}{\partial x}+\frac{\partial v}{\partial y}=0 \tag{1}$$

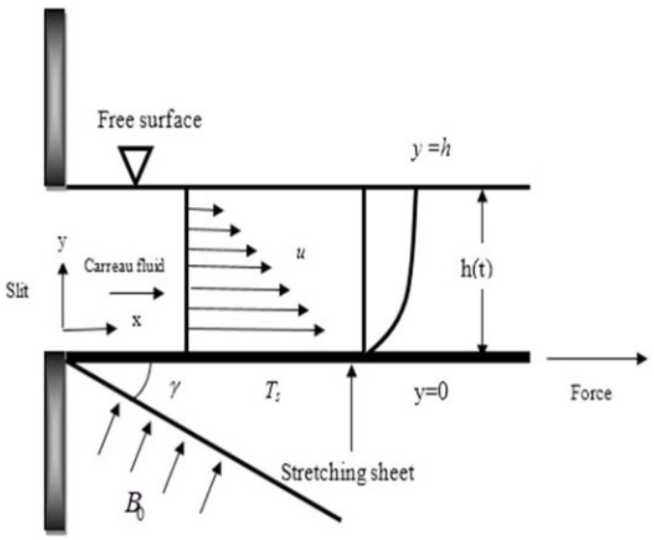

Fig. 1. Flow geometry of the problem [39]

$$\rho_{nf}\left(\frac{\partial u}{\partial t}+u\frac{\partial u}{\partial x}+v\frac{\partial u}{\partial y}\right)= \mu_{nf}\left(1+\frac{3(n-1)\Gamma^2}{2}\left(\frac{\partial u}{\partial y}\right)^2\right)\frac{\partial^2 u}{\partial y^2}-\sigma B_o^2 u\cos^2\gamma \tag{2}$$

$$\left(\rho c_p\right)_{nf}\left(\frac{\partial T}{\partial t}+u\frac{\partial T}{\partial x}+v\frac{\partial T}{\partial y}\right)= k_{nf}\frac{\partial^2 T}{\partial y^2}+\mu_{nf}\left(\frac{\partial u}{\partial y}\right)^2+q''' \tag{3}$$

where

$$\rho_{nf}=\rho_f(1-\phi)+\rho_s\phi \tag{4-a}$$

$$\left(\rho C_p\right)_{nf}=\left(\rho C_p\right)_f(1-\phi)+\left(\rho C_p\right)_s\phi \tag{4-b}$$

$$\mu_{nf}=\frac{\mu_f}{(1-\phi)^{2.5}} \tag{5}$$

$$k_{nf}=k_f\left[\frac{k_s+2k_f-2\phi(k_f-k_s)}{k_s+2k_f+\phi(k_f-k_s)}\right] \tag{6}$$

Assuming no slip condition, the appropriate boundary conditions are given as [39]

$$u=U_w,\quad v=0,\quad T=T_s \quad at \quad y=0 \tag{7-a}$$

$$\frac{\partial u}{\partial y}=0,\quad \frac{\partial T}{\partial y}=0,\quad y=h \tag{7-b}$$

$$v=\frac{dh}{dt}=-\frac{\alpha\beta}{2}\left(\frac{v_f}{b(1-\alpha t)}\right)^{\frac{1}{2}},\qquad y=h(t)=\beta\left(\frac{v_f(1-\alpha t)}{b}\right)^{\frac{1}{2}} \tag{8}$$

The non-uniform heat generation/absorption q''' is taken as

$$q'''=\frac{k_f U_w}{x v_f}\left[A^*(T_s-T_o)f'+B^*(T_s-T_o)\right] \tag{9}$$

where T_o is the ambient temperature and the surface temperature T_s of the stretching sheet varies with respect to distance x-from the slit as

$$T_s=T_o-T_{ref}\left(\frac{bx^2}{2v_f(1-at)^{\frac{3}{2}}}\right) \tag{10}$$

And the stretching velocity varies with respect to x as

$$U=\frac{bx}{(1-at)} \tag{11}$$

On introducing the following stream functions

$$u=\frac{\partial\psi}{\partial y},\quad v=\frac{\partial\psi}{\partial x} \tag{12}$$

And the similarity variables

$$u=\frac{bx}{(1-at)}f'(\eta,t),\qquad v=-(bv_f)^{-\frac{1}{2}}(1-at)^{-\frac{1}{2}}f(\eta,t),\qquad \eta=(b/v_f)^{\frac{1}{2}}(1-at)^{-\frac{1}{2}}y,\qquad T=T_o-T_{ref}\left(bx^2/2v_f\right)(1-at)^{-\frac{3}{2}}\theta(\eta) \tag{13}$$

Substituting Eqs. (12) and (13) into Eqs. (1) to (3), we have a partially coupled third and second orders ordinary differential equation

$$f'''\left\{1+\frac{3(n-1)We(f'')^2}{2}\right\} +B_1\left\{B_2\left(S\left(f'+\frac{\eta}{2}f''\right)+ff''-(f')^2\right)\right\} -Ha^2 f'cos^2\gamma=0 \tag{14-a}$$

$$B_3\theta''+\frac{EcPr}{B_1}(f'')^2+\left\{A^*f'+B^*\theta\right\} -B_4 Pr\left\{\frac{S}{2}\left((\eta\theta'+3\theta)+2f'\theta-f\theta'\right)\right\}=0 \tag{14-b}$$

where

$$
\begin{aligned}
&We^2=\frac{b^3x^2\Gamma^2}{v_f\left(1-at\right)^3},\quad Pr=\frac{\mu c_p}{k_f},\\
&Ha^2=\frac{\sigma B_o^2}{\rho_f b},\quad Ec=\frac{U_w^2}{c_p\left(T_s-T_0\right)},\\
&S=\frac{\alpha}{b},\quad R=\frac{4\sigma^* T_0^3}{k^* k_f}\\
&B_1=\left(1-\phi\right)^{2.5},\quad B_2=1-\phi+\phi\frac{\rho_s}{\rho_f},\\
&B_3=\frac{k_{nf}}{k_f},\quad B_4=1-\phi+\phi\frac{\left(\rho c_p\right)_s}{\left(\rho c_p\right)_f}
\end{aligned}
\tag{15}
$$

And the following boundary conditions becomes

$$
\begin{aligned}
&\eta=0,\quad f=0,\quad f'=1,\quad \theta=0\\
&\eta=\beta,\quad f=\frac{S\beta}{2},\quad f''=0,\quad \theta'=0
\end{aligned}
\tag{16}
$$

β indicates the value of the similarity variable η at the free surface so that η value gives

$$\eta=\left(b/v_f\right)^{\frac{1}{2}}\left(1-at\right)^{-\frac{1}{2}}h,$$

3- Solution Procedure

The nonlinearity in governing equation Eq. (14) makes it very difficult to develop a closed-form solution to the non-linear equation. Therefore, in this work, a spectral collocation method of the Chebyshev type is employed to solve the heat transfer equation. The Chebyshev collocation spectral method is based on the expansion by virtue of the Chebyshev polynomials. At first, it expands the variable at collocation points and seeks the variable derivatives at these points, then substitutes the expansions into the differential equations and finally seeks the approximated solution in physical space. This means that Chebyshev collocation spectral method is accomplished through, starting with Chebyshev approximation for the approximate solution and generating approximations for the higher-order derivatives through successive differentiation of the approximate solution.
Looking for an approximate solution, which is a global Chebyshev polynomial of degree N defined on the interval [-1, 1], the interval is discretized by using collocation points to define the Chebyshev nodes in [-1, 1], namely

$$x_j=cos\left(\frac{j\pi}{N}\right),j=0,1,2,...N \tag{17}$$

The derivatives of the functions at the collocation points are given by:

$$f^{n}\left(x_j\right)=\sum_{j=0}^{N}d_{kj}^{n}f\left(x_j\right),\quad n=1,2. \tag{18}$$

where d_{kj}^{n} represents the differential matrix of order n and are given by

$$d_{kj}^{1}=\frac{4\gamma_j}{N}\sum_{n=0,l=0}^{N}\ \sum_{n+l=odd}^{n-1}\frac{n\gamma_n}{c_l}T_l^{n}\left(x_k\right)T_n\left(x_j\right),\quad k,j=0,1,...N, \tag{19-a}$$

$$d_{kj}^{2}=\frac{2\gamma_j}{N}\sum_{n=0,l=0}^{N}\ \sum_{n+l=even}^{n-1}\frac{n\gamma_n\left(n^2-l^2\right)}{c_l}T_l^{n}\left(x_k\right)T_n\left(x_j\right),\quad k,j=0,1,...N, \tag{19-b}$$

where $T_n(x_j)$ are the Chebyshev polynomial and coefficients γ_j and c_l are defined as:

$$\gamma_j=\begin{cases}\frac{1}{2} & j=0,or\ N\\ \text{űűűű}\ j= & N-\end{cases} \tag{20-a}$$

$$c_l=\begin{cases}2 & l=0,or\ N\\ 1 & l=1,2,...N-1\end{cases} \tag{20-b}$$

As described above, the Chebyshev polynomials are defined on the finite interval [-1, 1]. Therefore, to apply Chebyshev spectral method to our Eq. (14), we make a suitable linear transformation and transform the physical domain [-1, 1] to Chebyshev computational domain [-1,1]. We sample the unknown function w at the Chebyshev points to obtain the data vector $w=[w(x_0), w(x_1), w(x_2), ... w(x_n)]^T$. The next step is to find a Chebyshev polynomial P of degree N that interpolates the data (*i.e.* $P(x_j)=w_j$, $j=0,1,...N$) and obtains the spectral derivative vector w by differentiating P and evaluating at the grid points (*i.e.* $w_j'=P'(x_j)=w_j$, $j=0,1,...N$). This transforms the nonlinear differential equation into system nonlinear algebraic equations, which are solved by Newton's iterative method starting with an initial guess.
Making a suitable transformation to map the physical domain [0, 1] to a computational domain [-1,1] to facilitate our computations.
Eq. (14) are transformed to the following equations

$$
\begin{aligned}
&\tilde{f}'''\left\{1+\frac{3\left(n-1\right)We\left(\tilde{f}''\right)^2}{2}\right\}\\
&+B_1\left\{B_2\left(S\left(\tilde{f}'+\frac{\eta}{2}\tilde{f}''\right)+\tilde{f}\tilde{f}''-\left(\tilde{f}'\right)^2\right)\right\}\\
&-Ha^2\tilde{f}cos^2\gamma=0
\end{aligned}
\tag{21-a}
$$

$$
\begin{aligned}
&B_3\tilde{\theta}''+\frac{EcPr}{B_1}\left(\tilde{f}''\right)^2+\left\{A^*\tilde{f}'+B^*\tilde{\theta}\right\}\\
&-B_4Pr\left\{\frac{S}{2}\left(\left(\eta\tilde{\theta}'+3\tilde{\theta}\right)+2\tilde{f}'\tilde{\theta}-\tilde{f}\tilde{\theta}'\right)\right\}=0
\end{aligned}
\tag{21-b}
$$

And the boundary conditions in Eq. (16) become

$$
\begin{aligned}
&\eta=0,\quad \tilde{f}=0,\quad \tilde{f}'=1,\quad \tilde{\theta}=0\\
&\eta=\beta,\quad \tilde{f}=\frac{S\beta}{2},\quad \tilde{f}''=0,\quad \tilde{\theta}'=0
\end{aligned}
\tag{22}
$$

After applying Chebyshev Spectral Collocation Method (CSCM) to Eq. (14) and the boundary conditions in Eq. (16), the governing equation and boundary conditions are transformed into a system of nonlinear algebraic equations:

$$\begin{aligned}&\sum_{j=0}^{N} d^{3}_{k,j}\tilde{f}\left(\eta_j\right)+\frac{3(n-1)}{2}We\left(\sum_{j=0}^{N} d^{(3)}_{k,j}\tilde{f}\left(\eta_j\right)\right)\left(\sum_{j=0}^{N} d^{(2)}_{k,j}\tilde{f}\left(\eta_j\right)\right)^2\\&+B_1B_2 s\left(\sum_{j=0}^{N} d^{(1)}_{k,j}\tilde{f}\left(\eta_j\right)\right)\left(\sum_{j=0}^{N} d^{(2)}_{k,j}\tilde{f}\left(\eta_j\right)\right)\\&+\frac{B_1B_2 s}{2}\sum_{j=0}^{N}\eta_j d^{(2)}_{k,j}\tilde{f}\left(\eta_j\right)+B_1B_2\left(\sum_{j=0}^{N}\tilde{f}\left(\eta_j\right)d^{(2)}_{k,j}\tilde{f}\left(\eta_j\right)\right)\\&-B_1B_2\left(\sum_{j=0}^{N} d^{(1)}_{k,j}\tilde{f}\left(\eta_j\right)\right)^2-Ha^2cos^2\gamma\sum_{j=0}^{N} d^{(1)}_{k,j}\tilde{f}\left(\eta_j\right)=0\end{aligned} \tag{23}$$

For k = 2, 3,...N-1

$$\begin{aligned}&B_3\sum_{j=0}^{N} d^{(2)}_{k,j}\tilde{\theta}\left(\eta_j\right)+\frac{EcPr}{B_1}\left(\sum_{j=0}^{N} d^{(2)}_{k,j}\tilde{\theta}\left(\eta_j\right)\right)^2\\&+A^*\sum_{j=0}^{N} d^{(1)}_{k,j}\tilde{f}\left(\eta_j\right)++B^*\sum_{j=0}^{N} d^{(1)}_{k,j}\tilde{\theta}\left(\eta_j\right)\\&-\frac{B_4Prs}{2}\sum_{j=0}^{N}\eta_j d^{(1)}_{k,j}\tilde{\theta}\left(\eta_j\right)-\frac{3Prs}{2}B_4\theta\left(\eta_j\right)\\&-2B_4Pr\sum_{j=0}^{N}\tilde{\theta}\left(\eta_j\right)d^{(1)}_{k,j}\tilde{f}\left(\eta_j\right)\\&+B_4Pr\sum_{j=0}^{N}\tilde{f}\left(\eta_j\right)d^{(1)}_{k,j}\tilde{\theta}\left(\eta_j\right)=0\end{aligned} \tag{24}$$

For k=1, 2, 3,...N-1

And the following boundary conditions in Eq. (16) become

$$\begin{aligned}&\tilde{f}\left(-1\right)=0,\quad \sum_{j=0}^{N} d^{(1)}_{0}\tilde{f}\left(\eta_j\right)=1,\quad \tilde{\theta}\left(-1\right)=0\\&\tilde{f}\left(1\right)=\frac{S\beta}{2},\quad \sum_{j=0}^{N} d^{(1)}_{N,j}\tilde{f}\left(\eta_j\right)=0,\quad \sum_{j=0}^{N} d^{(1)}_{N,j}\tilde{\theta}\left(\eta_j\right)=0\end{aligned} \tag{25}$$

The above system of nonlinear algebraic equation contains $3N$-2 equations for the unknown $\tilde{f}(\eta_j)$, i=1,2,3,...N-1 and $\tilde{\theta}(\eta_j)$,i=1,2,3,...N-1 is solved by Newton's method.

4- Results and Discussion

Tables 1 and 2 show the comparison of the results of Numerical Methods (NM) and that of CSCM. The obtained results using CSCM are in very good agreements with the results of the numerical method using Runge-Kutta coupled with Newton method as presented by Kumar et al. [39] The high accuracy of CSCM gives high confidence about validity of the method in providing solutions to the problem.

Also, the tables depict the effect of physical parameters on $f''(0)$ and $-\theta'(0)$ (for the Cu-kerosene and Ag- Kerosene nanofluids) which are the friction factor and local Nusselt number, respectively. As it can be seen from the tables that increasing values of the magnetic field parameter leads to decreasing values of the friction factor and heat transfer rate. An increase in the value of volume fraction of nanoparticles

Table 1. Physical parameter values of $f''(0)$ and $-\theta'(0)$ for Cu-Kerosene nanofluid

Ha	*ϕ*	*We*	*S*	*n*	*A**	*E*	*γ*	*NM* [39] $f''(0)$	*CSCM* $f''(0)$	*NM* [39] $-\theta'(0)$	*CSCM* $-\theta'(0)$
1								-0.800673	-0.800673	3.183502	3.183502
2								-0.951051	-0.951050	3.137925	3.137923
3								-1.077238	-1.077238	3.097322	3.097320
	0.1							-0.951051	-0.951050	3.137925	3.137923
	0.2							-0.926769	-0.926768	2.900338	2.900336
	0.3							-0.843920	-0.843921	2.683437	2.683437
		1						-0.865479	-0.865478	3.155764	3.155763
		3						-0.611938	-0.611938	3.218581	3.218581
		5						-0.484571	-0.484571	3.252867	3.252868
			0.2					-1.090240	-1.090238	3.094797	3.094797
			0.4					-1.002314	-1.002312	3.125135	3.125137
			0.6					-0.894041	-0.894040	3.149859	3.149861
				1				-0.995049	-0.995047	3.129665	3.129667
				5				-0.796797	-0.796798	3.171534	3.171534
				10				-0.700307	-0.700307	3.195477	3.195475
					1			-0.951051	-0.951050	3.002623	3.002622
					2			-0.951051	-0.951050	2.833496	2.833495
					3			-0.951051	-0.951050	2.664369	2.664368
						1		-0.951051	-0.951050	2.534955	2.534956
						2		-0.951051	-0.951050	1.864989	1.864989
						3		-0.951051	-0.951050	1.195023	1.195024
							π/6	-1.077238	-1.077237	3.097322	3.097321
							π/4	-0.951051	-0.951050	3.137925	3.137926
							π/3	-0.800673	-0.800673	3.183502	3.183501

Table 2. Physical parameter values of $f''(0)$ and $-\theta'(0)$ for Ag-Kerosene nanofluid

Ha	ϕ	*We*	*S*	*n*	*A**	*E*	γ	*NM* [39]	*CSCM*	*NM* [39]	*CSCM*
								$f''(0)$	$f''(0)$	$-\theta'(0)$	$-\theta'(0)$
1								-0.841593	-0.841595	-3.090642	-3.090644
2								-0.987394	-0.987396	-3.045404	-3.045403
3								-1.110328	-1.110327	-3.005010	-3.005011
	0.1							-0.987394	-0.987392	-3.045404	-3.045402
	0.2							-0.982125	-0.981227	-2.739717	-2.739718
	0.3							-0.907088	-0.907089	-2.473053	-2.473053
		1						-0.894212	-0.894211	-3.064925	-3.064924
		3						-0.627126	-0.627125	-3.132014	-3.132012
		5						-0.495591	-0.495590	-3.168031	-3.168030
			0.2					-1.133904	-1.133903	-2.982102	-2.982104
			0.4					-1.041797	-1.041795	-3.026448	-3.026447
			0.6					-0.926340	-0.926341	-3.063119	-3.063118
				1				-1.036497	-1.036498	-3.036220	-3.036221
				5				-0.820912	-0.820911	-3.081939	-3.081940
				10				-0.719234	-0.719235	-3.107549	-3.107547
					1			-0.987394	-0.987392	-2.906601	-2.906603
					2			-0.987394	-0.987392	-2.733098	-2.733096
					3			-0.987394	-0.987392	-2.559594	-2.559592
						1		-0.987395	-0.987394	-2.390294	-2.390293
						2		-0.987395	-0.987394	-1.662395	-1.662396
						3		-0.987395	-0.987394	-0.934497	-0.934497
							$\pi/6$	-1.110328	-1.110327	-3.005010	-3.005011
							$\pi/4$	-0.987394	-0.987395	-3.045404	-3.045406
							$\pi/3$	-0.841593	-0.841591	-3.090642	-3.090641

increases the friction factor and decreases the rate of heat transfer. Additionally, it is depicted as the value of aligned angle parameter increases, both friction factor and heat transfer rate increase. The Weissenberg and unsteadiness parameters have tendency to improve or enhance the rate of heat transfer.

The influence of pertinent parameters such as magnetic field parameter, unsteadiness parameter, heat source/sink parameter, Eckert number, volume fraction of nanoparticles etc. on the flow and heat transfer of the thin film flow are investigated.

Figs. 2 and 3 show the effects of magnetic field (*Ha*) on the velocity and temperature fields, respectively. It is revealed that there is a diminution in the velocity field and enhancement in the temperature field occur for increasing values of the Hartmann number *Ha*. This confirms the general physical behavior of the magnetic field that say that the fluid velocity depreciates for improved values of *Ha*. According to the physical point, Ha represents the ratio of electromagnetic force to the viscous force so large *Ha* implies that the Lorentz force increases, which is drag-like force that produces more resistance to transport phenomena due to which fluid velocity reduces. Consequently, the boundary layer thickness is a decreasing function of *Ha*, i.e. presence of magnetic field slows fluid motion at boundary layer and hence retards the velocity field. It should be noted that the magnetic field tends to make the boundary layer thinner, thereby increasing the wall friction. It is seen through Fig. 3 that the temperature profile $\theta(\eta)$ enhances increasing the Hartmann number *Ha*. Practically, the Lorentz force has a resistive nature which opposes motion of the fluid and as a result heat is produced which increases thermal boundary layer thickness and fluid temperature. The magnetic field tends to make the boundary layer thinner, thereby increasing the wall friction.

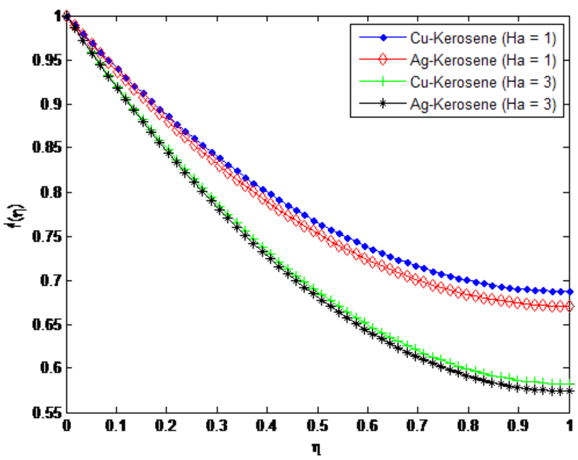

Fig. 2. Effect of Magnetic field parameter (Hartmann number) on the fluid velocity distribution

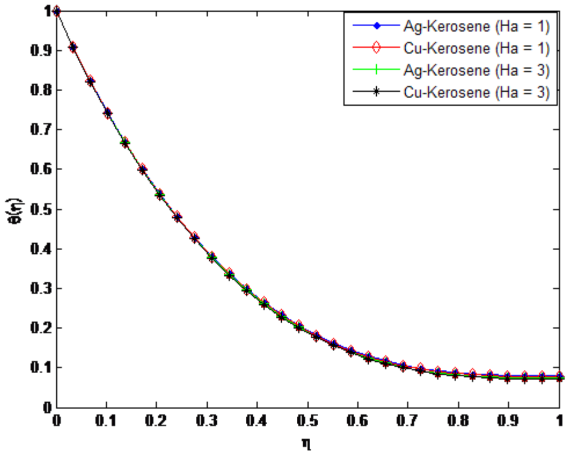

Fig. 3. Effect of Magnetic field parameter (Hartmann number) on the fluid temperature distribution

The effects of unsteadiness parameter on velocity and temperature profiles are shown in Figs. 4 and 5, respectively. It is observed that increasing values of S increases the velocity field while decreases the temperature field. This is because as the rate of heat loss by the thin film increases as the value of unsteadiness parameter increases.

Figs. 6 and 7 depict the effects of Weissenberg number (*We*) on the velocity and temperature profiles. It is shown from the figures that the velocity increases for increasing values of *We* and opposite trend was observed in temperature field. The observed trends in the velocity and temperature fields are due to the fact that a higher value of We will reduce the viscosity forces of the Carreau fluid. Increasing the Weissenberg number reduces the magnitude of the fluid velocity for shear thinning fluid while it arises for the shear thickening fluid. The influence of aligned angle on velocity profile is presented in Fig. 8. From the figure, it is shown that as the value of aligned parameter increases, the velocity field increases. It is due to the fact that with an increase in the angle of inclination, the effect of magnetic field on fluid particles decreases which reduces the Lorentz force. Consequently, the velocity profile increases. It is also noted that $\gamma = \pi/2$, the magnetic field has

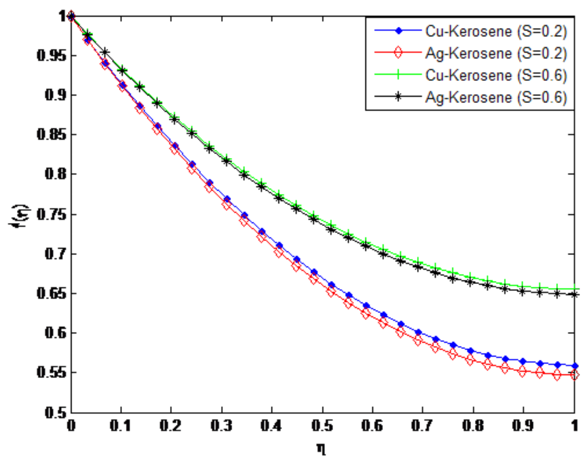

Fig. 4. Effect of unsteadiness parameter on the fluid velocity distribution

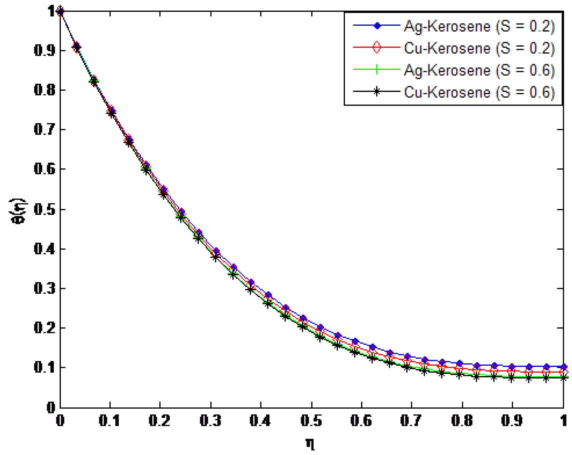

Fig. 5. Effect of unsteadiness parameter on the fluid temperature distribution

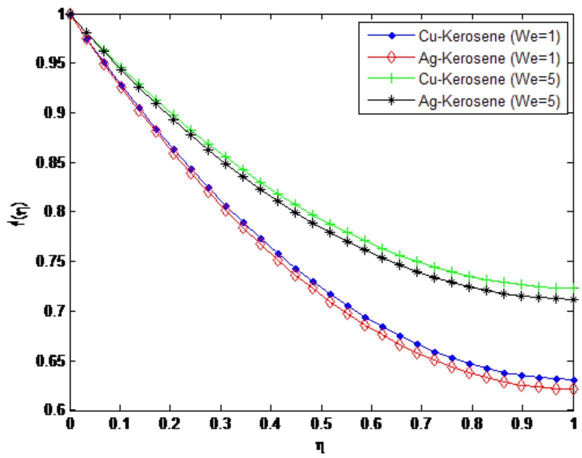

Fig. 6. Effect of Weissenberg number on the fluid velocity distribution

no effect on the velocity profile while maximum resistance is offered for the fluid particles when $\gamma = 0$. The influence of aligned angle on temperature profile $\theta(\eta)$ is shown in Fig. 9. It is analyzed that temperature profile is decreased by increasing aligned angle. Larger values of aligned angle result in smaller values of magnetic parameter which correspond to decrease in the restrictive force (Lorentz force). Hence, temperature profile decreases as the thermal boundary layer thickness is a direct function of magnetic field parameter.

Figs. 10 and 11 demonstrated the effect of power law index on velocity and temperature fields. As the power index is increased, it was observed that the velocity profile increases while the temperature profile decreases. This is because, increasing value of the power law index, thickens the liquid film associated with an increase of the thermal boundary layer. An increase in the momentum boundary layer thickness and a decrease in thermal boundary layer thickness is observed for the increasing values of the power law index including shear thinning to shear thickening fluids. Also, it should be pointed out that an increase in Weissenberg number correspond a decrease in the local skin friction coefficient and the magnitude of the local Nusselt number s decreases when the

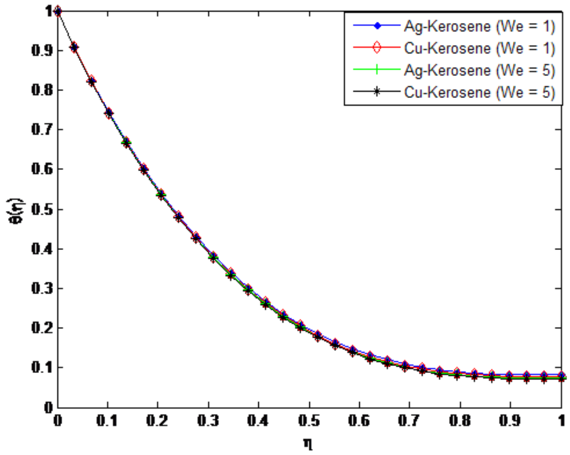

Fig. 7. Effect of Weissenberg number on the fluid temperature distribution

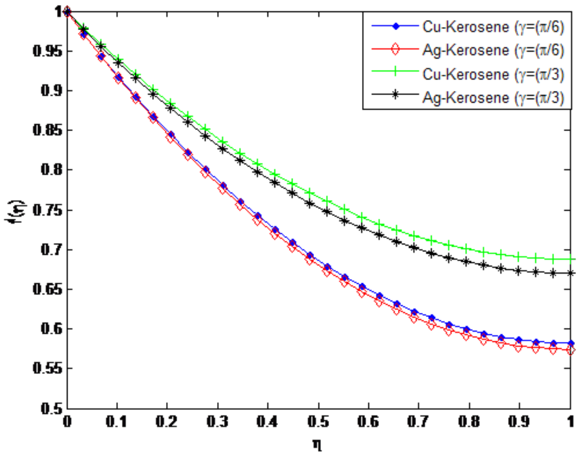

Fig. 8. Effect of aligned angle on the fluid velocity distribution

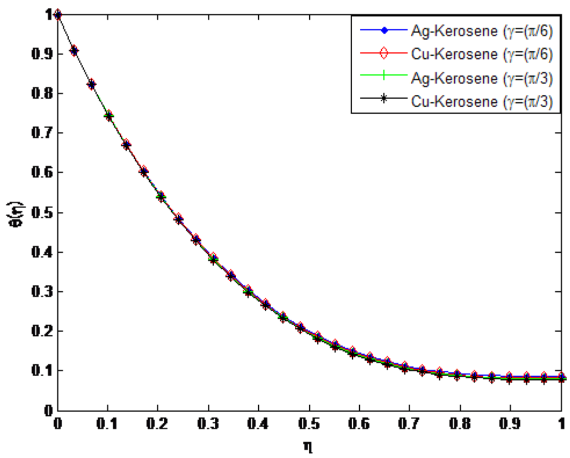

Fig. 9. Effect of aligned angle on the fluid temperature distribution

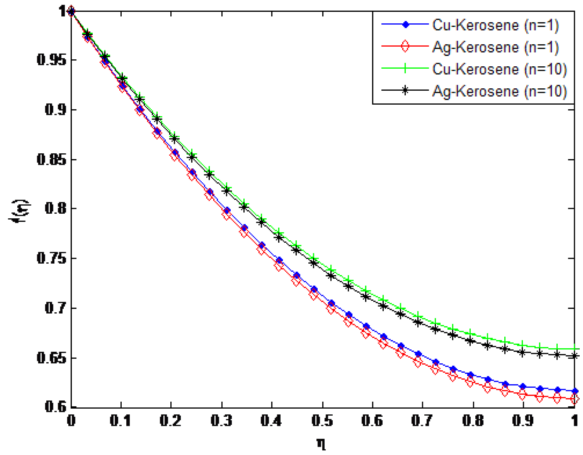

Fig. 10. Effect of power-law index on the fluid velocity distribution

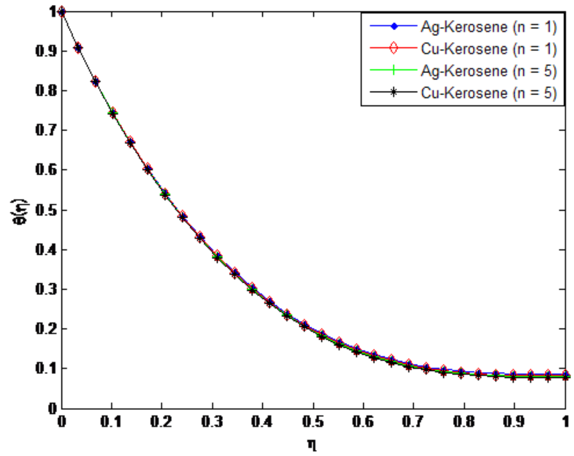

Fig. 11. Effect of power-law index on the fluid temperature distribution

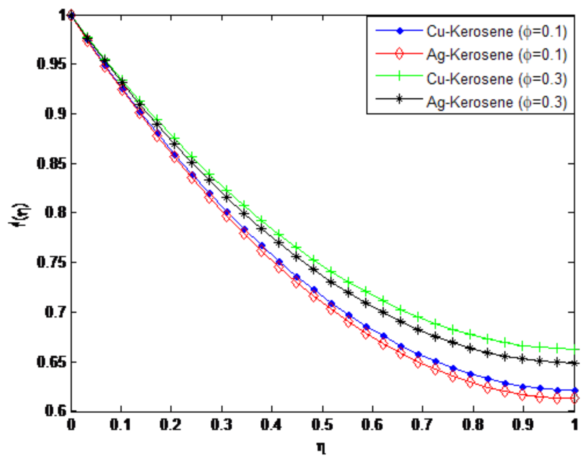

Fig. 12. Effect of nanoparticle volume fractions on the fluid velocity distribution

Weissenberg number increases. The effects of nanoparticles volume fraction on the velocity and temperature profiles are depicted in Figs. 12 and 13, respectively. The result shows that as the solid volume fraction of the film increases both the velocity and temperature field increases. This is because

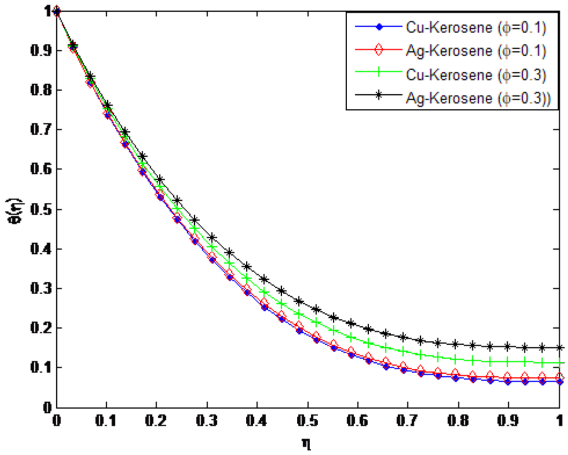

Fig. 13. Effect of nanoparticle volume fractions on the fluid temperature distribution

as the nanoparticle volume increases, more collision occurs between nanoparticles and particles with the boundary surface of the plate and consequently the resulting friction enhances the thermal conductivity of the flow and gives rise to increase the temperature within the fluid near the boundary region.
Figs. 14 and 15 depict the influence of non-uniform heat source/sink parameter on the temperature field. It is revealed that increasing the non-uniform heat source/sink parameter enhances the temperature fields. It is observed in the analysis that the temperature and thermal boundary layer thickness is depressed by increasing the Prandtl number, *Pr*. The effect of Eckert number on temperature profile is shown in Fig. 16. It was established that as the values of Eckert number increases, the values of the temperature distributions in the fluid increases. This is because as *Ec* increases, heat energy is saved in the liquid due to the frictional heating.

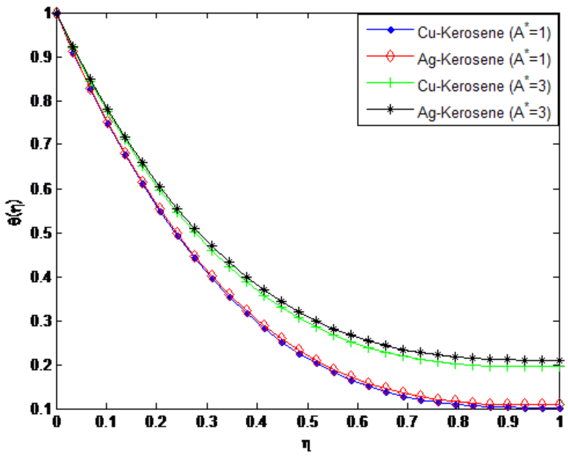

Fig. 14. Effect of non-uniform heat source/sink parameter (A^*) on the fluid temperature distribution

The effect of nanoparticle volume fraction ϕ on the film thickness of the nanofluid is shown in Fig. 17. It is evident from the figure that the film thickness is enhanced as the value of ϕ is increased. It can be inferred from Eq. (5) that if nanoparticle volume fraction ϕ is increased, the nanofluid viscosity will increased as there exist a direct relationship or proportion between the two parameters. As a result, the increasing viscosity resists the fluid motion along the stretching direction leading to the slowdown of the film thinning process.

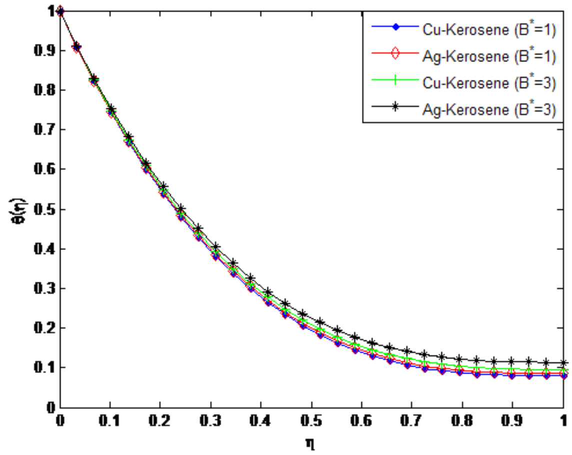

Fig. 15. Effect of non-uniform heat source/sink parameter (B^*) on the fluid temperature distribution

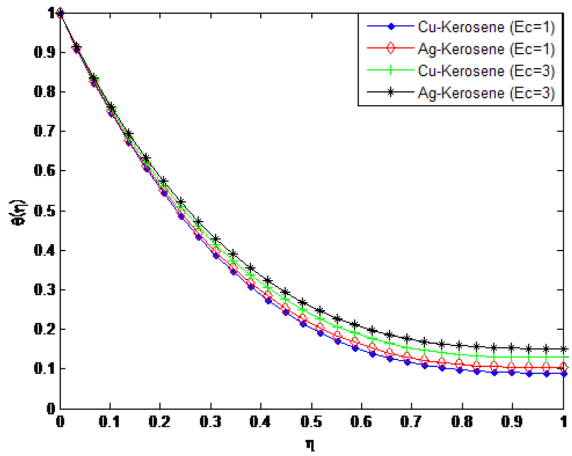

Fig. 16. Effect of Eckert number on the fluid temperature distribution

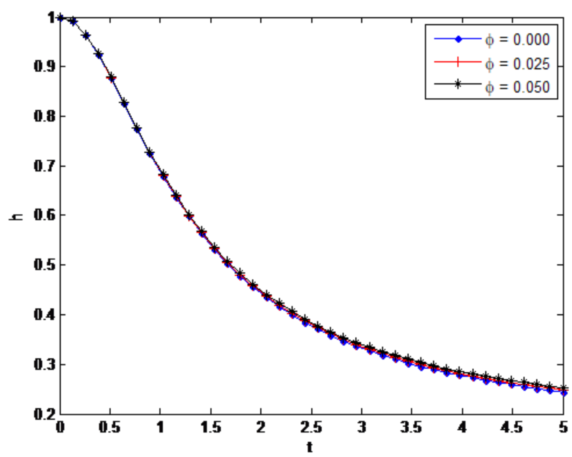

Fig. 17. Variation of film thickness h with time t for different values of ϕ

5- Conclusion

In this paper, Chebyshev spectral collocation method has been used to study the flow and heat transfer analyses of an electrically conducting liquid film flow Carreau nanofluid over a stretching sheet subjected to magnetic field, temperature dependent heat source/sink and viscous dissipation. The numerical solutions were verified Runge-Kutta coupled with Newton method. Using kerosene as the base fluid embedded with the silver (Ag) and copper (Cu) nanoparticles, the effects of pertinent parameters on reduced Nusselt number, flow and heat transfer characteristics of the nanofluid were investigated and discussed. From the results, it was established temperature field and the thermal boundary layers of Ag-kerosene nanofluid are highly effective when compared with the Cu-kerosene nanofluid. Thermal and momentum boundary layers of Cu-kerosene and Ag-kerosene nanofluids are not uniform. Heat transfer rate is enhanced by increasing in power-law index and unsteadiness parameter. Skin friction coefficient and local Nusselt number can be reduced by magnetic field parameter and they can be enhanced by increasing in aligned angle. Friction factor is depreciated and the rate of heat transfer increases by increasing the Weissenberg number. This analysis can help in expanding the understanding of the thermo-fluidic behaviour of the Carreau nanofluid over a stretching sheet.

Nomenclature

$\dot{a}$	time-dependent rate, /s
A^*	non-uniform heat generation/absorption parameter, W/m^3
B^*	non-uniform heat generation/absorption parameter, W/m^3
B_o	electromagnetic induction, kg/s^{2}A
C_p	specific heat capacity, J/kgK
Ec	Eckert number
h	height of the channel, m
M	Hartmann number/magnetic field parameter
n	power law index
q'''	non-uniform heat generation/absorption, W/m^3
Pr	Prandtl number
R	Radiation number
Re	permeation Reynolds number
S	unsteadiness parameter
t	time, s
T_s	surface temperature, K
T_o	ambient temperature, K
u	velocity component in x-direction, m/s
v	velocity component in y-direction, m/s
U_w	fluid inflow velocity at the wall, m/s
We	Weissenberg number
x	coordinate axis parallel to the channel walls, m
y	coordinate axis perpendicular to the channel walls, m

Greek symbol

ρ_{nf}	density of the nanofluid, kg/m^3
ρ_f	density of the fluid, kg/m^3
μ_{nf}	dynamic viscosity of the nanofluid, kg/ms
ρ_s	density of the nanoparticles, kg/m^3
ϕ	fraction of nanoparticles in the nanofluid
σ	electrical conductivity, S/m
Γ	time constant, s
γ	aligned angle, rad
θ	dimensionless temperature

References

[1] T. Hayat, I. Ullah, B. Ahmad, A. Alsaedi. Radiative flow of Carreau liquid in presence of Newtonian heating and chemical reaction. *Results in Physics* 7 (2017), 715–722.

[2] H. 1. Andersson, J. B. Aarseth, N. Braud and B. S. Dandapat. Flow of a Power-Law Fluid on an Unsteady Stretching Surface. *J. Non-Newtonian Fluid Mech.*, 62(1996), 1-8.

[3] H. I. Anderson, K. H. Bech, and B. S. Dandapat. Magneto Hydrodynamics Flow of a Power-Law Fluid Over A Stretching Sheet. *Int. J. Non- Linear Mech.* , 27(1992), 929-936.

[4] C. H. Chen. "Heat Transfer in a Power-Law Fluid Film over an Unsteady Stretching Sheet," *Heat Mass Transf. Und Stoffuebertragung*. 39(2003), 791–796.

[5] B. S. Dandapat, B. Santra and H. 1. Andersson. Thermo Capillarity in a Liquid Film on an Unsteady Stretching Surface. *Int. J. Heat and Mass transfer*, 46(2003), 3009-3015.

[6] B. S. Dandapat, B. Santra and K. Vejravelu. "The Effects of Variable Fluid Properties and the Thermo Capillarity on The Flow of a Thin Film On Stretching Sheet," *Int. J. Heat and Mass transfer*, 50(2007), 991-996.

[7] C. Wang. Analytic Solutions for a Liquid Film on an Unsteady Stretching Surface. *Heat Mass Transf. Und Stoffuebertragung*. 42(2006), 759– 766.

[8] C. H. Chen. Effect of Viscous Dissipation on Heat Transfer in a Non-Newtonian Liquid Film over an Unsteady Stretching Sheet," *J. Nonnewton. Fluid Mech.* 135(2206), 128–135.

[9] M. Sajid, T. Hayat and S. Asghar. Comparison between the HAM and HPM Solutions of Thin Film Flows of Non-Newtonian Fluids on a Moving Belt," *Nonlinear Dyn.* 50(2007), 27–35.

[10] B. S. Dandapat, S. Maity and A. Kitamura. "Liquid Film Flow Due to an Unsteady Stretching Sheet," *Int. J. Non. Linear. Mech.* 43(2008), 880–886.

[11] S. Abbasbandy, M. Yurusoy and M. Pakdemirli. The Analysis Approach of Boundary Layer Equation of Power-Law Fluids of Second Grade. *Zzeitschrift fur Naturforschung A*, 63(2008), 564-570.

[12] B. Santra and B. S. Dandapat. Unsteady Thin Film

Flow over A Heated Stretching Sheet," *Int. J. Heat. Mass transfer*, 52(2008), 1965-1970.

[13] M. Sajid, N. Ali and T. Hayat. On Exact Solutions for Thin Film Flows of A Micropolar Fluid. Commun. *Nonlinear Sci. Numer. Simul*. 14(2009), 451–461.

[14] N. F. M. Noor and I. Hashim. Thermocapillarity and Magnetic Field Effects in a Thin Liquid Film on an Unsteady Stretching Surface," *Int. J. Heat and mass Transfer*, 53(2010), 2044-2051.

[15] B. S. Dandapat and S. Chakraborty, S. "Effects of Variable Fluid Properties on Unsteady Thin-Film Flow over a Non-Linear Stretching Sheet," *Int. J. Heat Mass Transf.*, 53(2010), 5757–5763.

[16] B. S. Dandapat and S. K. Singh. "Thin Film Flow over a Heated Nonlinear Stretching Sheet in Presence of Uniform Transverse Magnetic Field," *Int. Commun. Heat Mass Transf.*, 38(2011), 324–328.

[17] G. M. Abdel-Rahman. Effect of Magnetohydrodynamic on Thin Films of Unsteady Micropolar Fluid through A Porous Medium," *J. Mod. Phys.*, 2(2011), 1290–1304.

[18] Y. Khan, Q. Wu, N. Faraz and A. Yildirim. The Effects of Variable Viscosity and Thermal Conductivity on a Thin Film Flow over a Shrinking/Stretching Sheet. *Comput. Math. with Appl.*, 61(2011), 3391– 3399.

[19] I. C. Liu, A. Megahed and H.H. Wang. "Heat Transfer in a Liquid Film due to an Unsteady Stretching Surface with Variable Heat Flux," *J. Appl. Mech.* , 80(2013), 1–7.

[20] K. Vajravelu, K. V. Prasad and C. O. Ng. Unsteady Flow and Heat Transfer in a Thin Film of Ostwald-De Waele Liquid Over A Stretching Surface. Commun. *Nonlinear Sci. Numer. Simul.* , 17(2012), 4163–4173.

[21] I.C. Liu and A. M. Megahed. Homotopy Perturbation Method for Thin Film Flow and Heat Transfer over an Unsteady Stretching Sheet with Internal Heating and Variable Heat Flux," *J. Appl. Math.*, 2012.

[22] R. C. Aziz, I. Hashim and S. Abbasbandy. "Effects of Thermocapillarity and Thermal Radiation on Flow and Heat Transfer In A Thin Liquid Film on an Unsteady Stretching Sheet," *Math. Probl. Eng.*, 2012.

[23] M. M. Khader and A. M. Megahed. Numerical Simulation Using The Finite Difference Method for the Flow and Heat Transfer in a Thin Liquid Film over an Unsteady Stretching Sheet in a Saturated Porous Medium in the Presence of Thermal Radiation. *J. King Saud Univ. - Eng. Sci.*, 25(2013), 29–34.

[24] Y. Lin, L. Zheng, X. Zhang, L. Ma and G. Chen. MHD Pseudo-Plastic Nanofluid Unsteady Flow And Heat Transfer In A Finite Thin Film Over Stretching Surface With Internal Heat Generation. *Int. J. Heat Mass Transf.*, 84(2015), 903–911.

[25] N. Sandeep, C. Sulochana and I. L. Animasaun. Stagnation Point Flow of a Jeffrey Nano Fluid over a Stretching Surface with Induced Magnetic Field and Chemical Reaction. *Int. J. Eng. Research in Afrika*, 20(2016), 93-111.

[26] J. Tawade, M. S. Abel, P. G. Metri and A. Koti, A.. "Thin Film Flow and Heat Transfer Over an Unsteady Stretching Sheet with Thermal Radiation, Internal Heating In Presence of External Magnetic Field," *Int. Adv. Appl. Math. And Mech.*,3(2016), 29-40.

[27] C. S. K. Raju and N. Sandeep. Unsteady three-dimensional flow of Casson-Carreau fluids past a stretching surface. *Alex Eng J.* 55(2016):1115–26.

[28] C. S. K. Raju and N. Sandeep. Falkner-Skan flow of a magnetic-Carreau fluid past a wedge in the presence of cross diffusion effects. *Eur Phys J Plus.* 131(2016), 267.

[29] C. S. K. Raju, N. Sandeep and V. Sugunamma. "Dual Solutions For Three-Dimensional MHD Flow Of A Nanofluid Over A Nonlinearly Permeable Stretching Sheet ," *Alexandria Engineering Journal*, 55(2016), 151162.

[30] N. Sandeep, O. K. Koriko and I. L. Animasaun, I.L. Modified Kinematic Viscosity Model for 3D-Casson Fluid Flow within Boundary Layer Formed On A Surface At Absolute Zero," *Journal of Molecular Liquids*, 221, 2016.

[31] M. J. Babu, N. Sandeep and C. S. K. Raju. Heat and Mass Transfer in MHD Eyring-Powell Nanofluid Flow Due To Cone in Porous Medium," *International Journal of Engineering Research in Africa*, 19(2106),57–74.

[32] I. L. Animasun, C. S. K. Raju and N. Sandeep, N. Unequal Diffusivities Case of Homogeneous-Heterogeneous Reactions within Viscoelastic Fluid Flow in the Presence of Induced Magnetic Field and Nonlinear Thermal Radiation," *Alexandria Engineering Journal*, 55(2)(2016),1595-1606.

[33] O. D. Makinde and I. L. Animasaun, I. L. Thermophoresis and Brownian Motion Effect on MHD Bioconvection of Nanofluid with Nonlinear Thermal Radiation and Quartic Chemical Reaction Past an Upper Horizontal Surface of A Paraboloid of Revolution. *J. of Mole. Liquids*, 221(2016), 733-743.

[34] O. D. Makinde and I. L. Animasaun. Bioconvection in MHD Nanofluid Flow with Nonlinear Thermal Radiation and Quartic Autocatalysis Chemical Reaction Past an Upper Surface of A Paraboloid Of Revolution," *J. of Ther. Sci.*, 109(2016), 159-171.

[35] N. Sandeep, N. Effect of Aligned Magnetic Field on Liquid Thin Film Flow of Magnetic-Nanofluid Embedded With Graphene Nanoparticles," *Advanced Powder Technology*, (in Press).

[36] J. V. Ramana Reddy, V. Sugunamma, N. Sandeep. "Effect Of Frictional Heating on Radiative Ferrofluid Flow over a Slendering Stretching Sheet With Aligned Magnetic Field," *Europen Physical Journal Plus* 132(2017), 7.

[37] M. E. Ali and N. Sandeep. Cattaneo-Christov Model for Radiative Heat Transfer of Magnetohydrodynamic Casson-Ferrofluid: A Numerical Study," *Results in Physics*, 7(2017), 21-30.

[38] P. J. Carreau. Rheological equations from molecular network theories. *Trans Soc Rheol.*, 116:99(1972)–127.

[39] M. S. Kumar, N. Sandeep, B. R. Kumar. Free convection Heat transfer of MHD dissipative Carreau Nanofluid Flow Over a Stretching Sheet. *Frontiers in Heat and Mass Transfer*, 813(2017).

[40] T. Hayat, N. Saleem, S. Asghar, M. S. Alhothuali, A. Alhomaidan A.. Influence of induced magnetic field and heat transfer on peristaltic transport of a Carreau fluid.

Commun Nonlinear Sci Numer Simul., 16(2011), 3559–77.

[41] B. I. Olajuwon B. I. Convective heat and mass transfer in a hydromagnetic Carreau fluid past a vertical porous plated in presence of thermal radiation and thermal diffusion. *Therm Sci.*, 15:241–52, 2011.

[42] T. Hayat , S. Asad, M. Mustafa, A. Alsaedi. Boundary layer flow of Carreau fluid over a convectively heated stretching sheet. *Appl Math Comput.*,246(2014):12–22.

[43] N. S. Akbar, S. Nadeem, U. I. Haq Rizwan, Ye Shiwei. MHD stagnation point flow of Carreau fluid toward a permeable shrinking sheet: Dual solutions. *Ain Shams Eng J.*, 5(2014):1233–9.

[44] N. S. Akbar, N. S. Blood flow of Carreau fluid in a tapered artery with mixed convection, *Int. J. Biomath*. 7 (6)(2014), 1450066–1450087.

[45] S. Mekheimer Kh,, F. Salama, M. A. El Kot. The unsteady flow of a carreau fluid through inclined catheterized arteries haveing a balloon with Time-Variant Overlapping Stenosis, *Walailak Journal of Science and Technology* (*WJST*) 12(2015), 863-883.

[46] Y. A. Elmaboud, K. S. Mekheimer, M. S. Mohamed M. S. Series solution of a natural convection flow for a Carreau fluid in a vertical channel with peristalsis. *J Hydrodyn Ser B*, 27(2015), 969–79.

[47] M. Hashim and Khan. A revised model to analyze the heat and mass transfer mechanisms in the flow of Carreau nanofluids. *Int J Heat Mass Transfer*, 103(2016),:291–7.

[48] G. R. Machireddy and S. Naramgari. Heat and mass transfer in radiative MHD Carreau fluid with cross diffusion. *Ain Shams Eng J* 2016.

[49] Sulochana C, Ashwinkumar GP, Sandeep N. Transpiration effect on stagnationpoint flow of a Carreau nanofluid in the presence of thermophoresis and Brownian motion. *Alex Eng J.* 55(2016), 1151–1157

[50] D. Gottlieb, S.A. Orszag, Numerical analysis of spectral methods: Theory and applications, in: *Regional Conference Series in Applied Mathematics*, *SIAM*, Philadelphia, 28(1977), 1–168.

[51] C. Canuto, M.Y. Hussaini, A. Quarteroni, T.A. Zang, *Spectral Methods in Fluid Dynamics*, Springer-Verlag, New York, 1988.

[52] R. Peyret, *Spectral Methods for Incompressible Viscous Flow*, SpringerVerlag, New York, 2002.

[53] F.B. Belgacem, M. Grundmann, Approximation of the wave and electromagnetic diffusion equations by spectral methods, *SIAM Journal on Scientific Computing* 20 (1) (1998), 13–32.

[54] X.W. Shan, D. Montgomery, H.D. Chen, Nonlinear magnetohydrodynamics by Galerkin-method computation, *Physical Review A* 44 (10) (1991), 6800–6818.

[55] X.W. Shan, Magnetohydrodynamic stabilization through rotation, *Physical Review Letters* 73 (12) (1994), 1624–1627.

[56] J.P. Wang, Fundamental problems in spectral methods and finite spectral method, *Sinica Acta Aerodynamica* 19 (2) (2001), 161–171.

[57] E.M.E. Elbarbary, M. El-kady, Chebyshev finite difference approximation for the boundary value problems, *Applied Mathematics and Computation* 139 (2003), 513–523.

[58] Z.J. Huang, and Z.J. Zhu, *Chebyshev spectral collocation method for solution of Burgers' equation and laminar natural convection in two-dimensional cavities*,Bachelor Thesis, University of Science and Technology of China, Hefei, 2009.

[59] N.T. Eldabe, M.E.M. Ouaf, Chebyshev finite difference method for heat and mass transfer in a hydromagnetic flow of a micropolar fluid past a stretching surface with Ohmic heating and viscous dissipation, *Applied Mathematics and Computation* 177 (2006), 561–571.

[60] A.H. Khater, R.S. Temsah, M.M. Hassan, A Chebyshev spectral collocation method for solving Burgers'-type equations, *Journal of Computational and Applied Mathematics* 222 (2008), 333–350.

[61] C. Canuto, M.Y. Hussaini, A. Quarteroni, T.A. Zang, *Spectral Methods in Fluid Dynamics*, Springer, New York, 1988.

[62] E.H. Doha, A.H. Bhrawy, Efficient spectral-Galerkin algorithms for direct solution of fourth-order differential equations using Jacobi polynomials, *Appl. Numer. Math.* 58 (2008), 1224–1244.

[63] E.H. Doha, A.H. Bhrawy, Jacobi spectral Galerkin method for the integrated forms of fourth-order elliptic differential equations, *Numer. Methods Partial Differential Equations* 25 (2009) 712–739.

[64] E.H. Doha, A.H. Bhrawy, R.M. Hafez, A Jacobi–Jacobi dual-Petrov–Galerkin method for third- and fifth-order differential equations, *Math. Computer Modelling* 53 (2011), 1820–1832.

[65] E.H. Doha, A.H. Bhrawy, S.S. Ezzeldeen, Efficient Chebyshev spectral methods for solving multi-term fractional orders differential equations, *Appl. Math. Model.* (2011) doi:10.1016/j.apm.2011.05.011.

Please cite this article using:

M. G. Sobamowo, L. O. Jayesimi, M. A. Waheed, Chebyshev Spectral Collocation Method for Flow and Heat Transfer in Magnetohydrodynamic Dissipative Carreau Nanofluid over a Stretching Sheet with Internal Heat Generation, *AUT J. Mech. Eng.*, 3(1) (2019) 3-14.

DOI: 10.22060/ajme.2018.14196.5712